

Supporting Information for

High-k dielectric screen-printed inks for mechanical energy harvesting devices

Hannah S. Leese^{a,b,†}, Miroslav Tejkl^c, Laia Vilar^d, Leopold Georgi^e, Hin Chun Yau^a, Noelia Rubio^a,
Elisenda Reixach^d, Jan Buk^c, Qixiang Jiang^f, Alexander Bismarck^f, Robert Hahn^{g,†} and Milo S. P.
Shaffer^{a,†}

a. Department of Chemistry, Imperial College London, London, SW7 2AZ, UK.

b. Materials for Health Lab, Department of Chemical Engineering, University of Bath, Bath, BA2 7AY, UK.

c. Pardam, Roudnice nad Labem, Czech Republic.

d. Eurecat, Parc Científic TecnoCampus, Mataró – Barcelona, Spain

e. Technische Universität Berlin, TiB4/2-1, Gustav-Meyer-Allee 25, 13355 Berlin, Germany

f. Institute of Materials Chemistry and Research, University of Vienna, Währinger Strasse 42, A-1090 Vienna, Austria

g. Fraunhofer IZM, Gustav-Meyer-Allee 25, 13355 Berlin, Germany

[†]email h.s.leese@bath.ac.uk, Robert.Hahn@izm.fraunhofer.de and m.shaffer@imperial.ac.uk

Additional Experimental Information, Figures and Tables

Table of Contents

Figure S1 SEM images of a,b) as-received commercial BTO spherical nanoparticles and c,d) as-produced BSTO nanofibers produced by Pardam.

Figure S2 XRD diffractograms of BTO-*s* and BSTO-*f* before and after functionalization with PMMA

Figure S3 High resolution TEM images of BSTO fibers before and after polymerization of MMA from the brominated surface. It was not possible to fully resolve the crystal structure post-functionalisation but much clearer to resolve in the BSTO-*f* which had already been treated with APS but before polymer grafting.

Figure S4 AFM images to assess the surface roughness of BSTO-*f*-PMMA-epoxy ($\phi=0.05$) printed dielectric films and drawn down dielectric films a) root mean square (RMS) ~ 28 nm using a 90T polyester screen mesh, b) RMS ~ 11 nm using a 110T polyester screen mesh and c) and RMS ~ 4 nm with areas of larger particulates when using a draw-down bar to create a dielectric film d) is a typical cross-section of the printed BSTO-*f*-PMMA dielectric films.

Figure S5 Mechanical energy harvesting device preparation; once the elastomer, spring element and printed dielectric are prepared they are a) cut into shape, b) folded in a concertina shape to integrate the conductive elastomer with the dielectric layer c) the wiring is soldered in place and d) packaged in a cell.

Table S1 Summary of dielectric loss and breakdown strength.

Table S2 Summary table of dielectric composites in literature where the ceramic ferroelectric filler is BTO or STO and functionalized with polymer. The values are also presented graphically in Figure 4 in the main manuscript.

References for Table S2

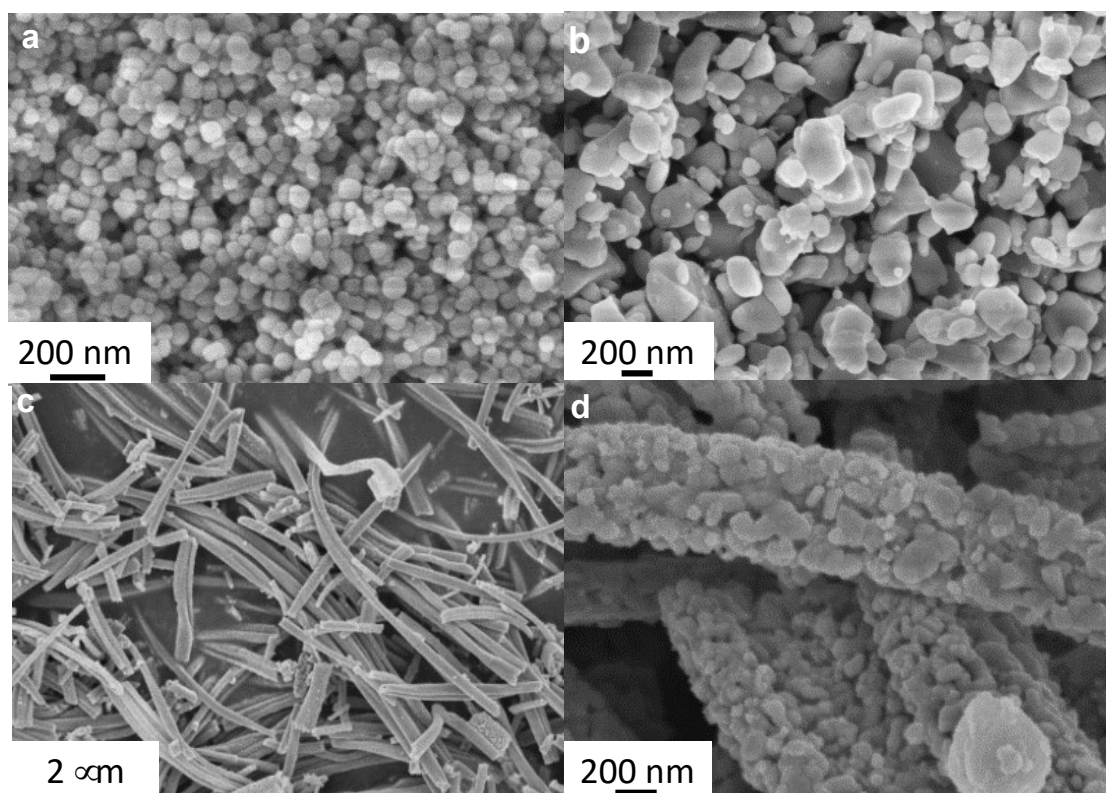


Figure S1 SEM images of a,b) as-received commercial BTO spherical nanoparticles and c,d) as-produced BSTO nanofibers produced by Pardam.

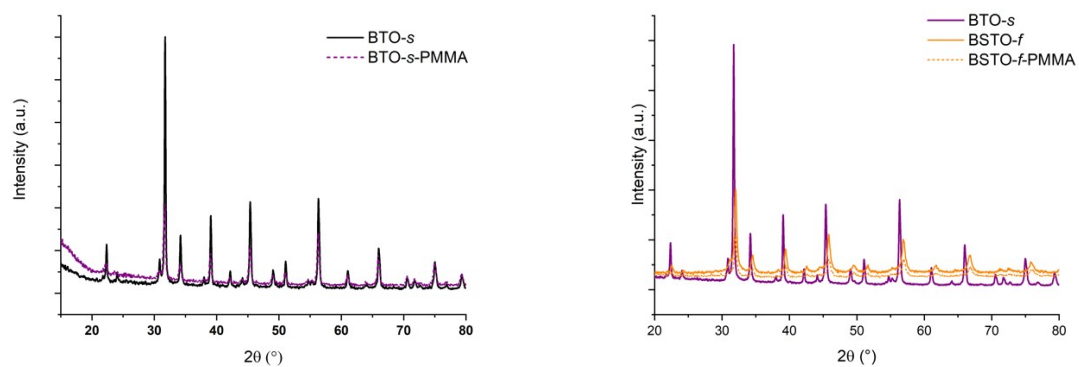


Figure S2 XRD diffractograms of BTO-*s* (**left**) and BSTO-*f* (**right**) before and after functionalization with PMMA

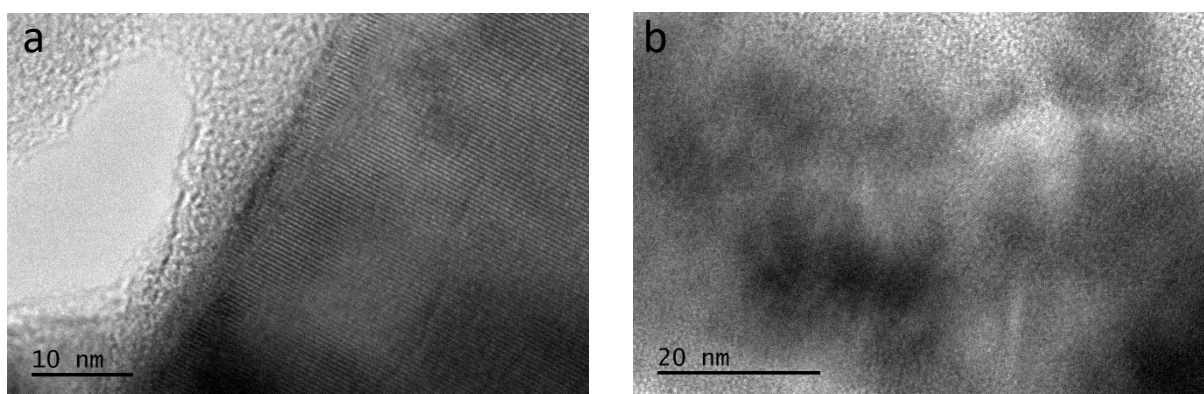


Figure S3 High resolution TEM images of BSTO fibers before a) and after b) polymerization of MMA from the brominated surface. It was not possible to fully resolve the crystal structure in the BSTO-*f* post-functionalisation b), but the lattice can be seen clearly in a) before polymer grafting.

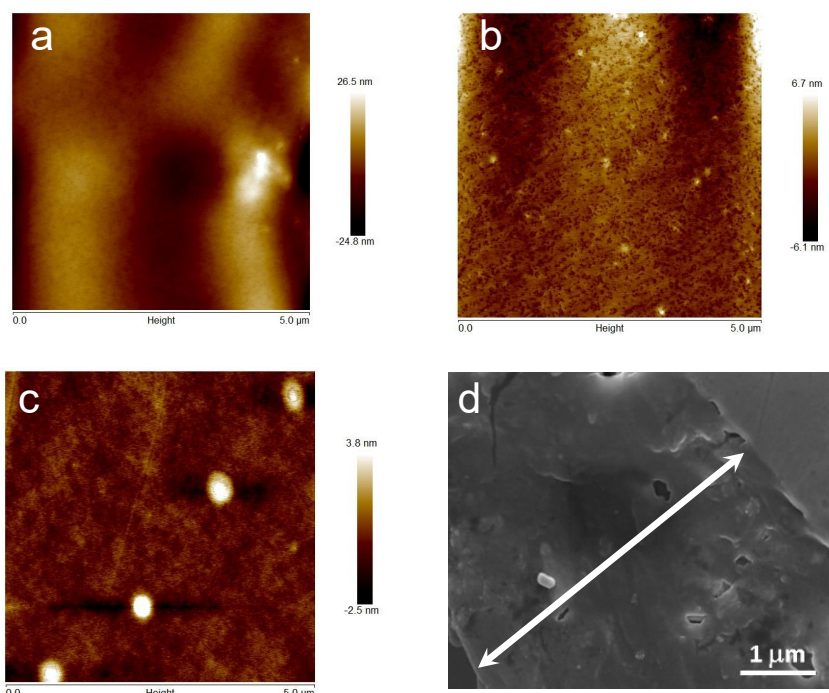


Figure S5 AFM images to assess the surface roughness of BSTO-*f*-PMMA-epoxy ($\phi=0.05$) printed dielectric films and drawn down dielectric films a) root mean square (RMS) ~ 28 nm using a 90T polyester screen mesh, b) RMS ~ 11 nm using a 110T polyester screen mesh and c) and RMS ~ 4 nm with areas of larger particulates when using a draw-down bar to create a dielectric film d) is a typical cross-section of the printed BSTO-*f*-PMMA dielectric films.

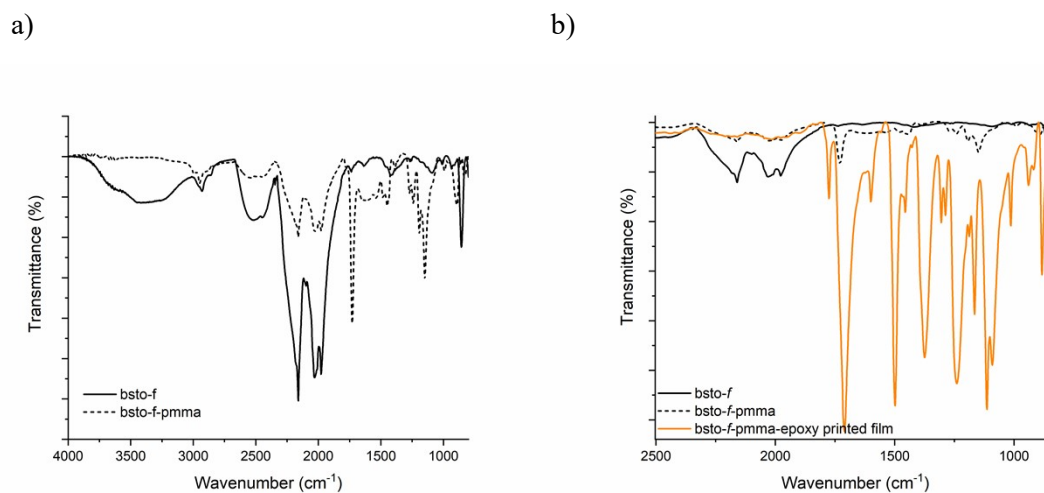


Figure S4 FTIR of a) BSTO-*f*, polymer functionalized BSTO-*f*-PMMA and b) the printed BSTO-*f*-PMMA-epoxy printed dielectric ink

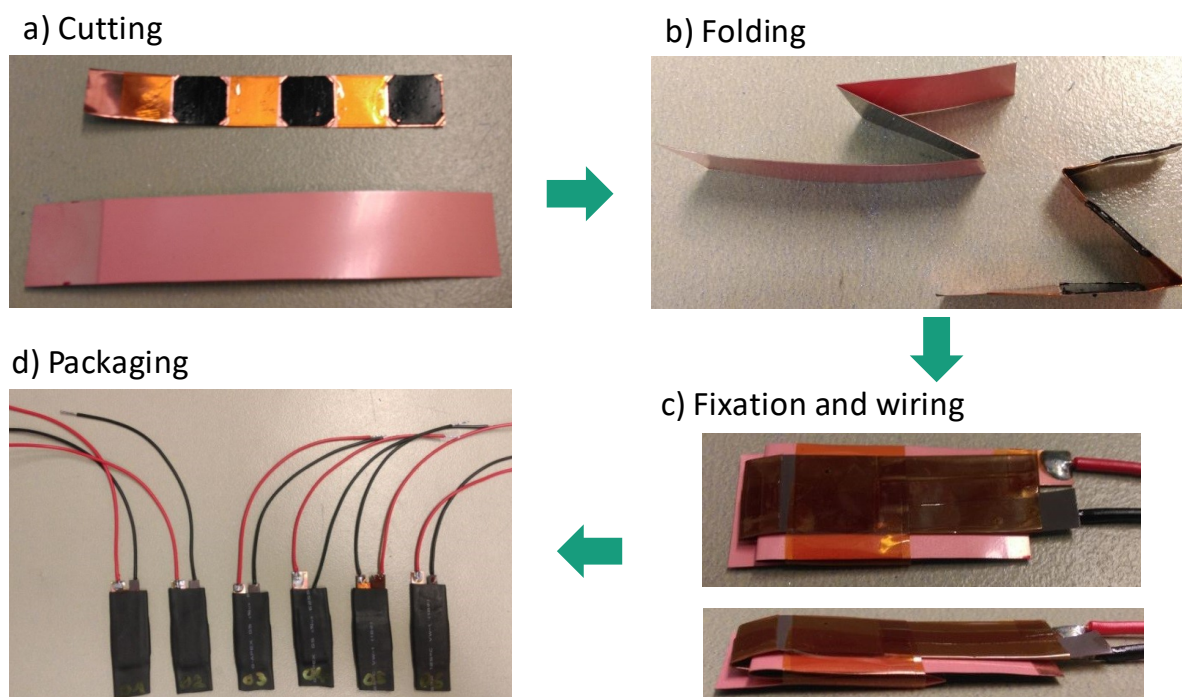


Figure S5 Mechanical energy harvesting device preparation; once the elastomer, spring element and printed dielectric are prepared they are a) cut into shape, b) folded in a concertina shape to integrate the conductive elastomer with the dielectric layer c) the wiring is soldered in place and d) packaged in a cell.

Table S1 Summary of dielectric loss and breakdown strength.

Printed sample	$\tan \delta^a$	Breakdown Strength ($\text{V } \mu\text{m}^{-1}$)
BSTO- <i>f</i> -PMMA-epoxy	0.10	103±18
BTO- <i>s</i> -PMMA-epoxy	0.20	100±20
Epoxy	0.50	220±10

^a. at 1kHz

Table S2 Summary table of dielectric composites in literature where the ceramic ferroelectric filler is BTO or STO and functionalized with polymer. The values are presented graphically in Figure 4 in the main manuscript document.

Ferroelectric Ceramic	Functionalised Polymer	Volume Fraction in composite	Frequency (kHz)	Dielectric Constant, ϵ	Ref.
BTO	PMMA	0.30	0.001	15	1
BTO	PMMA	0.65	0.01	100	2
BTO	PMMA	0.30	0.001	13	3
BTO (Zr)/PVP	PMMA	0.18	0.1	56	4
BTO-STO	PVDF	0.15	1	14.9	5

BTO	PVDF	0.20	0.1	30	6
BTO	PVDF	0.50	1	37	7
BTO	PVDF-HFP	0.50	1	43	8
BTO	PVDF-g-HEMA	0.20	1	75	9
BTO	PVDF-HFP	0.50	1	49	10
BTO (Zr)/PVP	PVDF	0.08	1	18	11
BTO fibres*	PVDF	0.20	0.001	23	12
STO fibres*	PVDF	0.10	1	18	13
BTO	HBP/PMMA	0.57	1	39	14
BTO	PS-b-P4VP(PDP)	0.50	1	32	15
BTO	PEN	0.05	0.1	9.5	16
BTO	Silane	0.60	0.1	52	17
BTO	PS	0.40	1	32	18
BTO	PS	0.59	1	33.1	19
BTO	PEDOT	0.25	1	25	20
BTO	PGMA	0.05	1	54	21
BTO	PHFDA	0.50	1	45	22
BTO	PDA/PLA	0.20	0.001	10	23

* Produced by electrospinning

References

1. L. Xie, X. Huang, C. Wu and P. Jiang, *Journal of Materials Chemistry*, 2011, **21**, 5897-5906.
2. K. Brandt, C. Neusel, S. Behr and G. A. Schneider, *Journal of Materials Chemistry C*, 2013, **1**, 3129-3137.
3. K. Hayashida, Y. Matsuoka and Y. Takatani, *RSC Advances*, 2014, **4**, 33530-33536.
4. V. S. Puli, M. Ejaz, R. Elupula, M. Kothakonda, S. Adireddy, R. S. Katiyar, S. M. Grayson and D. B. Chrisey, *Polymer*, 2016, **105**, 35-42.
5. D. Yu, N.-x. Xu, L. Hu, Q.-l. Zhang and H. Yang, *Journal of Materials Chemistry C*, 2015, **3**, 4016-4022.
6. F. Wen, Z. Xu, W. Xia, X. Wei and Z. Zhang, *Polymer Engineering & Science*, 2013, **53**, 897-904.
7. P. Kim, S. C. Jones, P. J. Hotchkiss, J. N. Haddock, B. Kippelen, S. R. Marder and J. W. Perry, *Advanced Materials*, 2007, **19**, 1001-1005.
8. L. Xie, X. Huang, K. Yang, S. Li and P. Jiang, *Journal of Materials Chemistry A*, 2014, **2**, 5244-5251.
9. M.-F. Lin and P. S. Lee, *Journal of Materials Chemistry A*, 2013, **1**, 14455-14459.
10. D. Zhang, Z. Wu, X.-f. Zhou, A.-q. Wei, C. Chen and H. Luo, *Sensors and Actuators A: Physical*, 2017, **260**, 228-235.
11. S. Liu, S. Xue, S. Xiu, B. Shen and J. Zhai, *Scientific Reports*, 2016, **6**, 26198.
12. X. Zhang, Y. Ma, C. Zhao and W. Yang, *Applied Surface Science*, 2014, **305**, 531-538.
13. L. Yao, Z. Pan, J. Zhai, G. Zhang, Z. Liu and Y. Liu, *Composites Part A: Applied Science and Manufacturing*, 2018, **109**, 48-54.
14. L. Xie, X. Huang, Y. Huang, K. Yang and P. Jiang, *The Journal of Physical Chemistry C*, 2013, **117**, 22525-22537.
15. K. H. Lee, J. Kao, S. S. Parizi, G. Caruntu and T. Xu, *Nanoscale*, 2014, **6**, 3526-3531.
16. Y. You, W. Han, L. Tu, Y. Wang, R. Wei and X. Liu, *RSC Advances*, 2017, **7**, 29306-29311.
17. M. Iijima, N. Sato, I. Wuled Lenggoro and H. Kamiya, *Colloids and Surfaces A: Physicochemical and Engineering Aspects*, 2009, **352**, 88-93.
18. D. Wang, M. Huang, J. Zha, J. Zhao, Z. Dang and Z. Cheng, *IEEE Transactions on Dielectrics and Electrical Insulation*, 2014, **21**, 1438-1445.
19. K. Yang, X. Huang, M. Zhu, L. Xie, T. Tanaka and P. Jiang, *ACS Applied Materials & Interfaces*, 2014, **6**, 1812-1822.

20. T. Wang, X. Zhang, D. Chen, Y. Ma, L. Wang, C. Zhao and W. Yang, *Applied Surface Science*, 2015, **356**, 232-239.
21. M. Ejaz, V. S. Puli, R. Elupula, S. Adireddy, B. C. Riggs, D. B. Chrisey and S. M. Grayson, *Journal of Polymer Science Part A: Polymer Chemistry*, 2015, **53**, 719-728.
22. K. Yang, X. Huang, Y. Huang, L. Xie and P. Jiang, *Chemistry of Materials*, 2013, **25**, 2327-2338.
23. Y. Fan, X. Huang, G. Wang and P. Jiang, *The Journal of Physical Chemistry C*, 2015, **119**, 27330-27339.